Noninvasive monitoring of tissue hemoglobin using UV-VIS diffuse reflectance spectroscopy: a pilot study

Janelle E. Bender,[1,*] Allan B. Shang,[2] Eugene W. Moretti,[2] Bing Yu,[1] Lisa M. Richards,[1] and Nirmala Ramanujam[1]

[1]*Department of Biomedical Engineering, Duke University, 136 Hudson Hall, Box 90281, Durham, NC 27708, USA*
[2]*Department of Anesthesiology, Duke University Medical Center, Box 3094, Durham, NC 27710, USA*
**janelle.bender@duke.edu*

Abstract: We conducted a pilot study on 10 patients undergoing general surgery to test the feasibility of diffuse reflectance spectroscopy in the visible wavelength range as a noninvasive monitoring tool for blood loss during surgery. Ratios of raw diffuse reflectance at wavelength pairs were tested as a first-pass for estimating hemoglobin concentration. Ratios can be calculated easily and rapidly with limited post-processing, and so this can be considered a near real-time monitoring device. We found the best hemoglobin correlations were when ratios at isosbestic points of oxy- and deoxyhemoglobin were used, specifically 529/500 nm. Baseline subtraction improved correlations, specifically at 520/509 nm. These results demonstrate proof-of-concept for the ability of this noninvasive device to monitor hemoglobin concentration changes due to surgical blood loss. The 529/500 nm ratio also appears to account for variations in probe pressure, as determined from measurements on two volunteers.

OCIS codes: (170.6510) Spectroscopy, tissue diagnostics; (170.1470) Blood or constituent monitoring.

References and links

1. G. A. Thibodeau, and K. T. Patton, *Anatomy and Physiology*, 5 ed. (Mosby, Inc., St. Louis, MO, 2003).
2. American Society of Anesthesiologists Task Force on Perioperative Blood Transfusion and Adjuvant Therapies, "Practice guidelines for perioperative blood transfusion and adjuvant therapies: an updated report by the American Society of Anesthesiologists Task Force on Perioperative Blood Transfusion and Adjuvant Therapies," Anesthesiology **105**(1), 198–208 (2006).
3. B. I. Whitaker, J. Green, M. R. King, L. L. Leibeg, S. N. Mathew, K. S. Schlumpf, and G. B. Schreiber, "The 2007 Nationwide Blood Collection and Utilization Survey Report," (US Department of Health and Human Services, 2007). *http://www.dhhs.gov/ophs/bloodsafety/2007nbcus_survey.pdf*.
4. M. R. Macknet, S. Norton, P. Kimball-Jones, and R. Applegate, "Continuous noninvasive measurement of hemoglobin via pulse CO-oximetry," Anesth. Analg. **104**, S-32 (2007).
5. M. R. Macknet, P. Kimball-Jones, R. Applegate, and M. Allard, "Continuous non-invasive measurement of hemoglobin via pulse CO-oximetry during liver transplantation, a case report," Anesth. Analg. **104**, S-31 (2007).
6. T. Ahrens, and K. Rutherford, *Essentials of oxygenation*, 1 ed. (Jones & Bartlett Publishers, Boston, MA, 1993).
7. J. W. McMurdy, G. D. Jay, S. Suner, and G. Crawford, "Noninvasive optical, electrical, and acoustic methods of total hemoglobin determination," Clin. Chem. **54**(2), 264–272 (2008).
8. W. Secomski, A. Nowicki, P. Tortoli, and R. Olszewski, "Multigate Doppler measurements of ultrasonic attenuation and blood hematocrit in human arteries," Ultrasound Med. Biol. **35**(2), 230–236 (2009).
9. R. O. Esenaliev, Y. Y. Petrov, O. Hartrumpf, D. J. Deyo, and D. S. Prough, "Continuous, noninvasive monitoring of total hemoglobin concentration by an optoacoustic technique," Appl. Opt. **43**(17), 3401–3407 (2004).
10. R. G. Nadeau, and W. Groner, "The role of a new noninvasive imaging technology in the diagnosis of anemia," J. Nutr. **131**(5), 1610S–1614S (2001).
11. D. A. Benaron, I. H. Parachikov, W.-F. Cheong, S. Friedland, B. E. Rubinsky, D. M. Otten, F. W. H. Liu, C. J. Levinson, A. L. Murphy, J. W. Price, Y. Talmi, J. P. Weersing, J. L. Duckworth, U. B. Hörchner, and E. L. Kermit, "Design of a visible-light spectroscopy clinical tissue oximeter," J. Biomed. Opt. **10**(4), 044005 (2005).

#117329 - $15.00 USD Received 16 Sep 2009; revised 6 Nov 2009; accepted 9 Nov 2009; published 7 Dec 2009

12. X. Wu, S. Yeh, T. W. Jeng, and O. S. Khalil, "Noninvasive determination of hemoglobin and hematocrit using a temperature-controlled localized reflectance tissue photometer," Anal. Biochem. **287**(2), 284–293 (2000).
13. S. Zhang, B. R. Soller, S. Kaur, K. Perras, and T. J. Vandersalm, "Investigation of noninvasive *in vivo* blood hematocrit measurement using NIR reflectance spectroscopy and partial least-squares regression," Appl. Spectrosc. **54**(2), 294–299 (2000).
14. J. W. McMurdy, G. D. Jay, S. Suner, F. M. Trespalacios, and G. P. Crawford, "Diffuse reflectance spectra of the palpebral conjunctiva and its utility as a noninvasive indicator of total hemoglobin," J. Biomed. Opt. **11**(1), 014019 (2006).
15. B. Yu, J. Y. Lo, T. F. Kuech, G. M. Palmer, J. E. Bender, and N. Ramanujam, "Cost-effective diffuse reflectance spectroscopy device for quantifying tissue absorption and scattering *in vivo*," J. Biomed. Opt. **13**(6), 060505 (2008).
16. J. Y. Lo, B. Yu, H. L. Fu, J. E. Bender, G. M. Palmer, T. F. Kuech, and N. Ramanujam, "A strategy for quantitative spectral imaging of tissue absorption and scattering using light emitting diodes and photodiodes," Opt. Express **17**(3), 1372–1384 (2009).
17. M. J. Rathbone, *Oral Mucosal Drug Delivery*. (Marcel Dekker, Inc., New York, NY, 1996).
18. G. M. Palmer, and N. Ramanujam, "Monte Carlo-based inverse model for calculating tissue optical properties. Part I: Theory and validation on synthetic phantoms," Appl. Opt. **45**(5), 1062–1071 (2006).
19. G. M. Palmer, C. Zhu, T. M. Breslin, F. Xu, K. W. Gilchrist, and N. Ramanujam, "Monte Carlo-based inverse model for calculating tissue optical properties. Part II: Application to breast cancer diagnosis," Appl. Opt. **45**(5), 1072–1078 (2006).
20. J. E. Bender, K. Vishwanath, L. K. Moore, J. Q. Brown, V. Chang, G. M. Palmer, and N. Ramanujam, "A robust Monte Carlo model for the extraction of biological absorption and scattering *in vivo*," IEEE T. Biomed. Eng. (N.Y.) **56**(4), 960–968 (2009).
21. K. Vishwanath, H. Yuan, W. T. Barry, M. W. Dewhirst, and N. Ramanujam, "Using optical spectroscopy to longitudinally monitor physiological changes within solid tumors," Neoplasia **11**(9), 889–900 (2009).
22. K. Vishwanath, D. Klein, K. Chang, T. Schroeder, M. W. Dewhirst, and N. Ramanujam, "Quantitative optical spectroscopy can identify long-term local tumor control in irradiated murine head and neck xenografts," J. Biomed. Opt. **14**(5), 054051 (2009).
23. Q. Liu, and N. Ramanujam, "Scaling method for fast Monte Carlo simulation of diffuse reflectance spectra from multilayered turbid media," J. Opt. Soc. Am. A **24**(4), 1011–1025 (2007).
24. S. Prahl, "Optical Properties Spectra," (Oregon Medical Laser Center, 2003). *http://omlc.ogi.edu/spectra/index.html*.
25. R. Reif, M. S. Amorosino, K. W. Calabro, O. A'Amar, S. K. Singh, and I. J. Bigio, "Analysis of changes in reflectance measurements on biological tissues subjected to different probe pressures," J. Biomed. Opt. **13**(1), 010502 (2008).
26. Y. Ti, and W. C. Lin, "Effects of probe contact pressure on *in vivo* optical spectroscopy," Opt. Express **16**(6), 4250–4262 (2008).
27. E. Chan, B. Sorg, D. Protsenko, M. O'Neil, M. Motamedi, and A. Welch, "Effects of compression on soft tissue optical properties," IEEE J. Sel. Top. Quant. **2**(4), 943–950 (1996).
28. B. R. Duling, and C. Desjardins, "Capillary hematocrit – what does it mean?" News Physiol. Sci. **2**, 66–69 (1987).
29. R. D. Braun, M. W. Dewhirst, and D. L. Hatchell, "Quantification of erythrocyte flow in the choroid of the albino rat," Am. J. Physiol. **272**(3 Pt 2), H1444–H1453 (1997).
30. M. G. Mythen, and A. R. Webb, "Intra-operative gut mucosal hypoperfusion is associated with increased post-operative complications and cost," Intensive Care Med. **20**(2), 99–104 (1994).

1. Introduction

Hemoglobin (Hb) levels in humans range from 12 to 16 g/dl [1]. Blood transfusions are indicated when Hb reaches between 6 and 10 g/dl and are also dependent upon signs of organ ischemia, the patient's intravascular volume status, and the presence of other patient risk factors [2]. In addition to Hb concentration measurements, blood pressure, heart rate, temperature, and blood oxygen saturation are commonly included in the assessment of whether or not to transfuse [2]. Over 14 million transfusions were given to approximately 5 million people in the United States alone in 2006 [3]. The current strategy for monitoring Hb concentration in the surgical setting is to procure a blood sample for laboratory analysis. Typically this is drawn from an indwelling arterial catheter that remains in the artery throughout surgery. This process is subject to human error, including mislabeling, specimen loss or mishandling, and it potentially exposes personnel to blood borne pathogens. Additionally, it is invasive and time-consuming and can thus cause a significant delay in determining the need for transfusion. For surgeries with a known potential for rapid and

#117329 - $15.00 USD Received 16 Sep 2009; revised 6 Nov 2009; accepted 9 Nov 2009; published 7 Dec 2009

significant hemorrhage a real-time, non-invasive monitoring device of total Hb would be of great benefit.

The instrument closest to being commercialized is the Masimo Corporation's SpHb monitor. This noninvasive Hb monitor has recently received FDA clearance (2008) and been initiated for full market release (2009). The SpHb monitor is a pulse oximeter which utilizes more than seven wavelengths of light which propagate through the fingertip. Details on the algorithm and wavelengths used are proprietary. The system has been validated in 19 surgical patients and 9 volunteers undergoing hemodilution yielding Hb concentrations ranging from 4.4 to 15.8 g/dl with a correlation coefficient of r=0.898 when compared to arterial Hb concentration [4]. Feasibility for monitoring total Hb for concentrations between 5.8 and 10.3 g/dl with the SpHb monitor has been carried out in a single liver transplant case, with a reported precision of 0.74 g/dl [5]. Pulse oximetry measures only arterial saturation and cannot be used in applications where the blood flow is non-pulsatile, such as during cardiac bypass surgery [6]. Several other techniques based on optical, optoacoustic, and ultrasound methods have been proposed to non-invasively measure total Hb. McMurdy, et al. provides a thorough review of these methods [7]. Ultrasonic attenuation measured non-invasively from the brachial artery has been shown to correlate with arterial hematocrit ranging from 32.0 to 49.3% with absolute mean error of 3.24% and standard deviation of 3.27% [8]. Optoacoustic methods have been tested in healthy volunteers via non-invasive measurements of the radial artery, but further development of sophisticated algorithms is required for accurate *in vivo* measurements of Hb [9]. In addition, the effects of skin pigmentation on optoacoustic measurements were not addressed. Optical polarization imaging studies have been shown to accurately separate normal versus anemic patients (12.0 g/dl cut-off) based on measurements from the sublingual mucosa with a correlation coefficient of r=0.93 for predicted versus reference Hb measured from venipuncture from the forearm. However, because polarization measurements of vessel segment density have no direct analog in existing laboratory measures, the clinical viability of this technique is still unclear [10].

Several studies have used visible (VIS) or VIS-near-infrared (NIR) diffuse reflectance spectroscopy to measure Hb concentration [11–14]. The Spectros T-Stat® is an FDA-approved VIS light spectroscopy device sensitive to ischemia [11]. The T-Stat® reports Hb saturation and concentration, but to the best of our knowledge only saturation has been validated *in vivo*. Another study tested the effect of calibration populations for anemia screening in blood donors using VIS-NIR temperature-controlled photometer measurements from the forearm [12]. In that study, the one anemic donor out of 19 donors was identified, but the estimates of Hb were affected by the skin pigmentation of the calibration population. In a different study utilizing NIR reflectance measurements from the forearm of cardiac bypass patients with hematocrit ranging from 14.3 to 44.2%, a correlation coefficient of r=0.71 was achieved when compared to arterial Hb [13]. However, skin pigmentation was again found to be a largely contributing factor to the predictive ability of this technique. Another study tested diffuse reflectance measurements at VIS wavelengths from the mucosal inner lining of the eyelid for use as a rapid anemia screening device in patients with Hb ranging from 7.3 to 16.7 g/dl [14]. There was a tradeoff in sensitivity and specificity for detecting anemia, depending on whether partial least-squares (PLS) or discrete region modeling analysis was used. With PLS, the sensitivity and specificity were 86% and 91%, while the discrete region model yielded 57% and 100%, respectively, indicating the importance of exploring these models further. While most of the studies described here exhibited good *in vivo* correlations of optical or acoustic parameters to total Hb and hematocrit, they typically are only useful for measurements of arterial saturations [4,5,8], require sophisticated algorithms [8,9,14] or have shown significant inter-patient variability due to skin pigmentation in the cases where measurements were made through the intact skin [12,13]. This presents an opportunity to explore new approaches that can address all three of these issues.

#117329 - $15.00 USD Received 16 Sep 2009; revised 6 Nov 2009; accepted 9 Nov 2009; published 7 Dec 2009

The focus of the pilot study reported here was to test the feasibility of monitoring Hb in surgical patients using a fiber probe-based diffuse reflectance spectroscopy system. Diffuse reflectance spectra reflect tissue absorption and scattering. The primary absorbers in soft tissues are oxygenated and deoxygenated Hb (oxy- and deoxy-Hb, respectively). Further, diffuse reflectance spectroscopy measures a mixture of venous and arterial components and does not require pulsatile blood flow. Additionally, diffuse reflectance systems have the flexibility to be made cost-effective and portable for use in a clinical setting [15-16]. In this study, a total of 36 concurrent optical and arterial blood gas (ABG) measurements of Hb from 10 patients undergoing major surgeries (where blood loss was expected) were used to assess the feasibility of a simple ratiometric method based on diffuse reflectance spectroscopy for noninvasive measurements of total Hb. The tissue surface chosen for placement of the probe was the floor of the mouth, a highly vascular and perfused mucosal surface that can be directly accessed by the fiber-optic probe. Although the sensing depth using diffuse reflectance spectroscopy in the VIS spectral range is shallow, it is well suited for use in the sublingual space, where the thickness of mucosal epithelium of the floor of the mouth is approximately 190 μm [17]. The correlations between optically-measured ratios of tissue diffuse reflectance intensities at wavelengths between 350 and 600 nm and arterial blood Hb obtained from ABG measurements were evaluated. The isosbestic reflectance ratio of 529/500 nm was shown to correlate well with blood Hb concentration (r=-0.66), and marked improvements were seen when baseline-subtracted data was used (r=-0.75). Additionally, the ratio at 520/509 nm was correlated to Hb concentration with r=-0.61 and baseline-subtracted comparisons improved the correlation to r=-0.84. The effect of probe pressure on the diffuse reflectance measurements was also tested in two volunteers. These studies demonstrated that reflectance ratios are less influenced by probe pressure than absolute reflectance intensities themselves. The initial findings from the study serve as proof-of-concept of a simple ratiometric method based on diffuse reflectance spectroscopy to measure non-pulsatile Hb concentrations directly from the oral mucosa.

2. Materials and methods

2.1. Patient study

Twenty patients undergoing surgery at the Duke University Medical Center (Durham, North Carolina) were enrolled in this study. This study was conducted according to a protocol approved by the Duke University IRB and with the patient's informed consent. Two probes with the same fiber geometries were used. The first probe was used in a total of 15 patients, but after the fifth patient, it was observed that there were cracked fibers, and so the subsequent 10 patients measured with the defective probe were discarded from the analysis. The second identically configured probe was used on five additional patients, and the integrity of the probe was maintained throughout the study. Thus only patients in whom probe integrity was maintained (the first five patients with the first probe and the five patients with the second probe) were included in the analysis. The details about the surgery type and the ABG measurements for those 10 patients are given in Table 1.

Patients were typically on at least 50% oxygen while receiving anesthesia. After the patient was anesthetized, the anesthesiologist placed the sterilized fiber optic probe inside the patient's mouth, flush against the sublingual tissue. In most cases, the probe was taped to the endotracheal or nasogastric tube to stabilize against movement. In the first patient, the probe was taped directly to the side of the patient's mouth. For seven of the ten patients, the probe had to be either replaced or slightly readjusted during the procedure to ensure contact with the tissue. If the probe was dislodged during the surgery, as judged by the shape of the reflectance spectra, the anesthesiologist repositioned the probe as close to the original position as possible. During the course of the surgery, optical measurements were taken approximately

#117329 - $15.00 USD Received 16 Sep 2009; revised 6 Nov 2009; accepted 9 Nov 2009; published 7 Dec 2009

every 15 minutes in duplicate or triplicate. When an ABG blood draw was taken, optical measurements were concurrently collected.

Table 1. Overview of surgery type, number of ABG and optical measurements during the time the probe was in place and range of ABG Hb (Hgb) levels

Patient	*Surgery Type*	*# ABG*	*# Optical*	*Hgb range (g/dl)*
1	Anterior spinal fixation	4	68	8.2-12.4
2	Radical hysterectomy	3	62	10.1-12.3
3	Liver resection	7	111	4.5-15.3
4	Exploratory laparotomy	3[†]	60[†]	8.7-12.0
5	Cervical spinal fusion	2	31	12.2-12.5
6	Pancreas whipple	4	96	10.9-13.1
7	Hernia	3	43	11.0-14.4
8	Abdominal aortic aneurysm	3	17	9.0-12.3
9	Bile duct resection	2	27	10.0-11.0
10	Radical prostatectomy	6	96	6.2-13.5

[†]The first seven optical measurements were taken before the probe was properly placed; one of the ABGs was during this time, so that optical-ABG data point was not included in analysis.

2.2 Optical measurements

Diffuse reflectance spectroscopy measurements in this study were performed using a SkinSkan (JY Horiba, Edison, NJ) spectrophotometer consisting of a 150 W xenon arc lamp and double-grating excitation monochromator as the wavelength-tunable source and an emission monochromator and extended red photomultiplier tube (PMT) on the collection end. The instrument was connected to a laptop computer. The SkinSkan, although a fluorometer, has been extensively used for diffuse reflectance spectroscopy studies of tissues [18–22]. The illumination and collection light was coupled to the tissue via a bifurcated fiber optic probe bundle (Romack, Inc., Williamsburg, VA) custom-designed in-house. The probe consisted of an 18-fiber collection ring around a 19-fiber illumination core. Each fiber had a core diameter of 200 μm with numerical aperture (NA) of 0.22. The probe was 5 m in total length, 4 m of which was enclosed in Teflon coating, making it fairly flexible. The common end of the probe, which was placed on the measurement surface, was surrounded by a stainless steel ferrule (3.72 mm diameter, 5 mm length).

The instrument was allowed to warm up for at least 15 minutes prior to beginning of the measurements. The PMT high voltage was fixed at 250 V. For each optical measurement, the diffuse reflectance was collected from 350 to 600 nm, in 5 nm increments (51 data points). The integration time per data point was 0.1 s for all measurements. The excitation and emission monochromator gratings were 1200 grooves/mm, and the slit widths were 0.5 mm, which resulted in a fixed 5 nm excitation bandpass. At the beginning or end of a set of measurements, the diffuse reflectance from a Spectralon reflectance standard (SRS-99-010, Labsphere, Inc., North Sutton, NH) was measured using the same instrument settings to record the day to day variations in instrument throughput.

2.3 Sensing depth simulations

The sensing depth above which 90% of the photons visited was calculated using Monte Carlo simulations [23] using wavelength-dependent optical properties representative of soft tissues in the UV-VIS wavelength range [20]. The probe geometry was simplified to a central illumination core with radius 0.055 cm surrounded by the 18 collection fibers. For each collection fiber, the radius and center-to-center distance to the illumination core was determined from an image of the common end of the probe. The NA was set to 0.22. The anisotropy factor, g, was assumed to be 0.8. The index of refraction was set to 1.45 for the fibers and 1.37 for the tissue. The simulation used five million photons and a homogeneous medium with thickness and radius of 3 cm, divided into grids of 0.01 cm (depth) x 3 cm (radial). The simulation records the visiting history, exit weight, and maximum depth for each photon detected by the collection fibers.

#117329 - $15.00 USD Received 16 Sep 2009; revised 6 Nov 2009; accepted 9 Nov 2009; published 7 Dec 2009

2.4 Data analysis

Ratios of all numerator-denominator pairs from 350 to 600 nm were tested as simple correlates to Hb concentration. Correlations were tested in Matlab using Pearson's linear correlation coefficients, under the assumption that the data was normally distributed. The spectra were interpolated to a 1 nm increment using a cubic spline interpolation prior to calculating the ratios, to increase the number of wavelength combinations. Ratios were obtained from raw reflectance spectra.

2.5 Tissue-probe interfacing

The effect of probe pressure was tested in sub-studies using two volunteers. The probe was placed inside a rubber tubing on which the volunteer bit lightly to hold the probe in place. Also surrounding the probe (within the rubber tubing) was a clear sheath to ensure additional security. The clear sheath extended past the rubber tubing and was clamped to the probe at the other end for each measurement. The probe tip was not covered by the tubing or sheath. The security of the probe in the volunteer measurements was designed to be comparable to that of the clinical measurements, where the probe was taped in. The probe was positioned on the sublingual tissue of a volunteer, and the operator varied the pressure between "light," "medium," and "hard." The pressure was qualitative, where the volunteer motioned when they felt like the pressure change was significant. For each pressure change, the clamp was secured on the clear sheath for the duration of the measurements. Measurements were taken from both the right and left side of the sublingual tissue, and each side was measured a second time after the probe was removed then replaced (Right 1, Right 2, Left 1, Left 2). Once the probe was replaced on a given side, it was situated with approximately the same starting pressure. Duplicate measurements were taken for each placement of the probe per site.

3. Results

3.1 Patient study

A total of 36 paired optical-ABG measurements were obtained from 10 patients (Table 1). Figure 1 shows the tissue diffuse reflectance spectra divided by the reflectance spectra of the standard for a single patient. The corresponding ABG Hb values are shown in the legend.

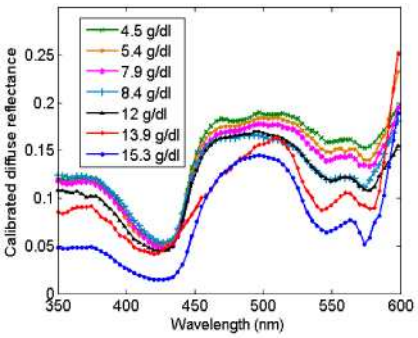

Fig. 1. Calibrated diffuse reflectance from patient #3 with corresponding ABG Hb values.

Correlations between all reflectance ratio pairs between 350 and 600 nm and ABG Hb values were tested. Figure 2(a) shows a correlation grid for all ratios over 350-600 nm. Each point on the grid represents a ratio or numerator-denominator pair. The numerator and denominator are indicated by the y- and x-axis, respectively. The color map indicates the absolute value of the Pearson's linear correlation coefficient between given ratios and the corresponding ABG Hb concentrations. Isosbestic points indicate where the molar extinction coefficients for the two species are equal. Over the wavelength range of 350-600 nm, there are eight isosbestic points for oxy- and deoxy-Hb: 390, 422, 452, 500, 529, 545, 570, and 584

#117329 - $15.00 USD Received 16 Sep 2009; revised 6 Nov 2009; accepted 9 Nov 2009; published 7 Dec 2009

nm [24], which are indicated by the axes labels in Fig. 2. The regions with the best correlations of optical ratios to ABG Hb (r>±0.65) were where the numerator was between 524 and 537 nm and the denominator between 482 and 507 nm. For numerators of 474-475 nm and denominators of 466-467 nm, the correlations were equally good (r>±0.65). The reverse case where the numerator was 466-467 nm and the denominator was 474-475 nm also had r>±0.65. The best correlation was at 532/499 nm, which correlated to ABG Hb with r=0.67. The ratio of 532/499 nm is close to the isosbestic ratio of 529/500 nm, which had r=-0.66. Because the correlation coefficients were so similar for both these ratios, the ratio 529/500 nm was retained.

Baseline-subtracted correlations were also tested, where the reflectance ratio for all wavelength pairs and the ABG Hb values measured at baseline were subtracted for all subsequent values for each patient. This is referred to as the delta ratio (and likewise delta ABG Hb) and was calculated as $\Delta\text{Ratio}(1:n-1) = \text{Ratio}(2:n) - \text{Ratio}(1)$ where n refers to the total number of measurements for a given patient. Correlations were then calculated between the delta reflectance ratios and delta ABG Hb values (Fig. 2(b)). For numerators ranging from 519 to 522 nm and 508-510 nm and corresponding denominator ranges of 507-511 nm and 519-521 nm respectively, the delta correlations had r>±0.8. The ratio that had the best correlation was 520/509 nm, with r=-0.84. The nearest isosbestic points in this range are 529 and 500 nm, which correlated to delta ABG Hb with r =–0.75 for 529/500 nm. The non-delta 520/509 nm correlation with ABG Hb was r=-0.61. The raw and delta correlations have similar patterns, but delta comparisons show stronger correlations with ABG values.

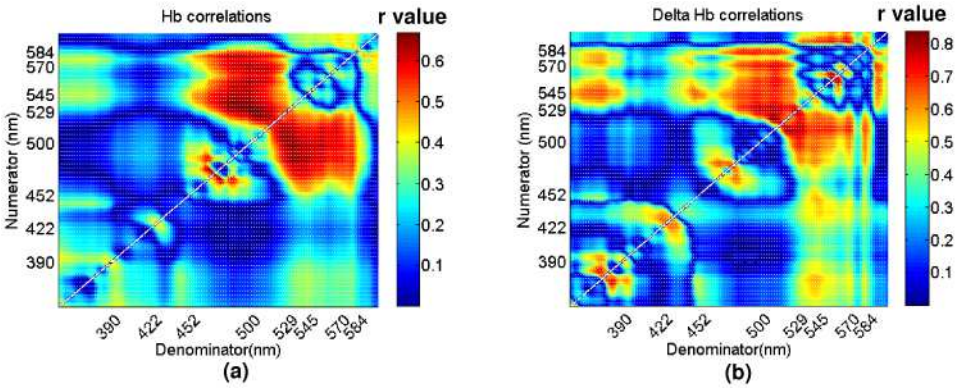

Fig. 2. Grid of r values (absolute value) for (a) non-delta and (b) delta reflectance ratios for all patients.

Figure 3 shows correlations between the 529/500 nm reflectance ratio and ABG Hb for both (a) non-delta and (b) delta comparisons plus correlations of (c) non-delta and (d) delta 520/509 nm reflectance ratio with ABG Hb data for all patients. The p-values represent the test of the hypothesis of no correlation against nonzero correlation. The black lines represent the best linear fit to the data; y=-0.01x+0.5 for non-delta 529/500 nm, y=-0.009x+0.01 for delta 529/500 nm, y=-0.008x+0.75 for non-delta 520/509, and y=-0.006x+0.002 for delta 520/509, where x refers to ABG Hb and y refers to the reflectance ratio. The slopes for all ratios are similar. The root mean square errors (RMSE) for non-delta and delta comparisons using 529/500 nm were both 0.03, and the RMSE for non-delta and delta 520/509 nm were 0.03 and 0.01, respectively. RMSE was calculated as the square root of the average squared distance between the measured optical ratios and the value predicted from the linear regression.

#117329 - $15.00 USD Received 16 Sep 2009; revised 6 Nov 2009; accepted 9 Nov 2009; published 7 Dec 2009

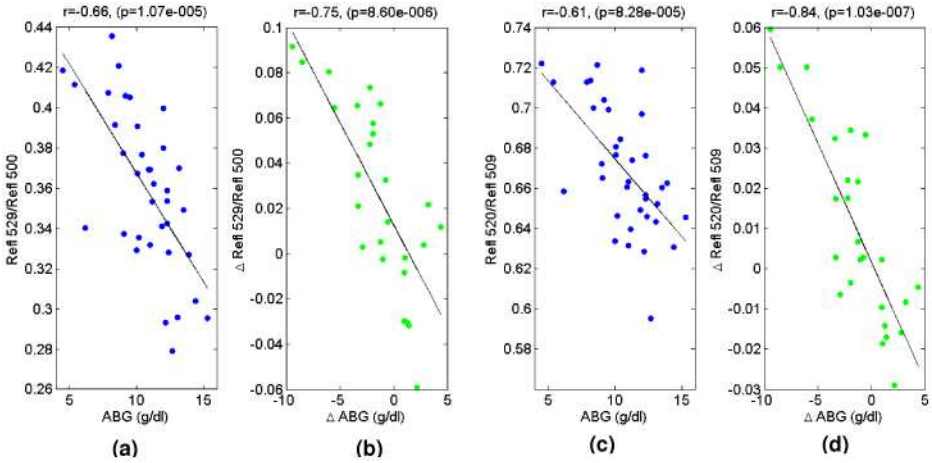

Fig. 3. Correlations of (a) non-delta 529/500, (b) delta 529/500, (c) non-delta 520/509, and (d) delta 520/509 nm with ABG Hb.

Figure 4 shows an example of the feasibility for this technique to monitor patient optical parameters over time. Figure 4(a) shows 529/500 nm (left y axis; solid line) and ABG Hb (right y axis; circles) for one patient. The reflectance ratio is seen to track the ABG Hb measurements during the period of blood loss. Because blood gases were taken only at seven points, the true Hb value is not known for the intermediate time points. Additionally, the anesthesia record only includes an estimate of blood loss at one time point, whereas the loss actually occurs over a period of time. Figure 4(b)-4(c) shows the baseline-subtracted delta comparisons for the same patient for (b) 529/500 nm and (c) 520/509 nm. The delta comparisons seem to match better, suggesting correction for some systematic offset with the non-delta ratios.

#117329 - $15.00 USD Received 16 Sep 2009; revised 6 Nov 2009; accepted 9 Nov 2009; published 7 Dec 2009

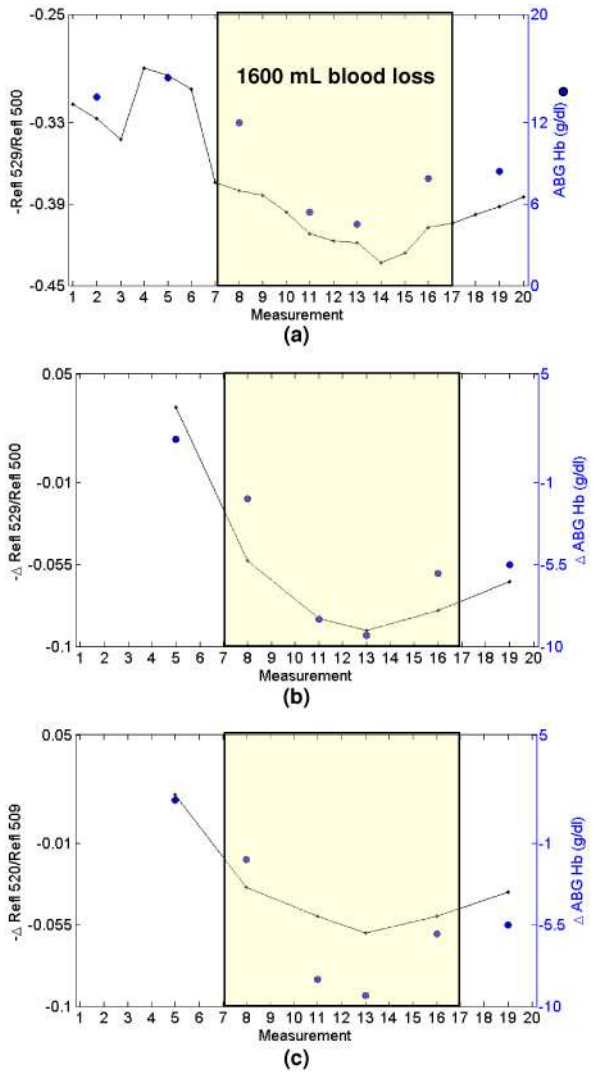

Fig. 4. (a) Optical monitoring of the 529/500 nm reflectance ratio over time for patient #3. The ratio is shown as negative because of the negative correlation between ABG Hb and the ratio; comparison between (b) delta 529/500 nm and (c) delta 520/509 nm reflectance ratios and delta ABG Hb for the same patient.

3.2. Sensing depth simulations

The 90% sensing depth averaged over 500 and 529 nm was calculated based on the weighted visiting frequency as a function of depth and is shown below in Table 2. The sensing depth is sufficiently large to probe beyond the epithelial mucosa of the floor of the mouth (~190 μm) but well within the thickness of the floor of the mouth.

Table 2. Wavelength-dependent 90% sensing depth calculated using absorption (μ_a) and reduced scattering (μ_s') coefficients shown below

Wavelength (nm)	*Sensing depth (mm)*	μ_a (cm^{-1})	μ_s' (cm^{-1})
500	1.8	0.78	8.15
529	1.5	1.42	7.99

#117329 - $15.00 USD Received 16 Sep 2009; revised 6 Nov 2009; accepted 9 Nov 2009; published 7 Dec 2009

3.3 Tissue-probe interfacing

Because pressure could not be controlled in the clinical study, the effect of probe pressure on the 529/500 nm ratio was tested in two volunteers (Volunteer 1 and 2). Two sites (right and left) on the sublingual tissue were each tested twice (Right 1, Right 2, Left 1, Left 2), with three qualitative pressures per site. For Volunteer 1, the probe accidentally moved on the second scan for high pressure of site Right 2, so only the first scan was considered. Figure 5(a1)-(a2) shows the reflectance standard-calibrated diffuse reflectance spectra from Right 1 for both volunteers. Ratios were calculated from the raw diffuse reflectance spectra. Figure 5b1-b2 shows the 529/500 nm ratio and Fig. 5c1-c2 shows the 520/509 nm ratio for each of the sites per volunteer, where the bars are in order of duplicate measurements of light, medium, and high pressure, as indicated for the first site. Based on this preliminary data, the 529/500 and 520/509 nm ratios are less susceptible to changes between low and medium pressure than the raw reflectance data, as there were no significant differences between low and medium pressure for either ratio. High pressure requires a lot of effort, and so the fact that there were statistically significant differences between low/medium and high pressure for several of the sites measured is not a significant concern. During the patient study, best efforts were made to maintain a low to medium pressure and avoid high pressures since that would be painful to the patient's mouth.

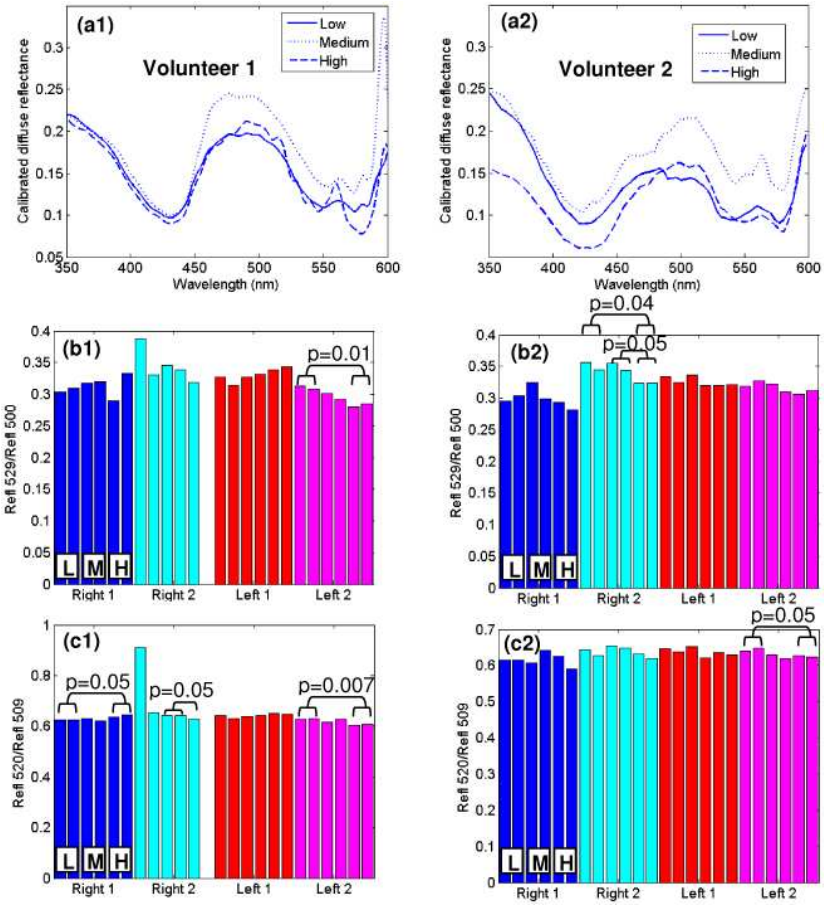

Fig. 5. (a1,a2) Diffuse reflectance from the first measurement of Right 1; (b1,b2) 529/500 nm reflectance ratio and (c1,c2) 520/509 nm reflectance ratio per volunteer; colors correspond to sites. Per site, there were three qualitative pressures: light, medium, and high, shown for Right 1. Measurements were made in duplicate per pressure per site.

#117329 - $15.00 USD Received 16 Sep 2009; revised 6 Nov 2009; accepted 9 Nov 2009; published 7 Dec 2009

3.4 Simulations

Monte Carlo simulations were carried out to test the effect of a range of Hb concentrations and saturations on the 529/500 nm isosbestic ratio. Total Hb was varied from 4 to 35 μM with Hb saturations from 25 to 100% and then used to calculate the absorption coefficient (μ_a) at 529 and 500 nm, using the molar extinction coefficients for each species [24]. Table 3 gives the concentrations of oxy- and deoxy-Hb with corresponding total Hb and Hb saturation. The reduced scattering coefficient (μ_s') was kept constant at 8.15 and 7.99 cm^{-1} for 529 and 500 nm, respectively (based on values in Table 2). The simulations were set up as described in Section 2.3, except one million photons were used. The Monte Carlo simulations [23] reported the diffuse reflectance collected by one collection fiber at 529 and 500 nm, which was then used to calculate the reflectance ratio. Figure 6 shows the reflectance ratio plotted as a function of (top) total Hb and (bottom) Hb saturation. The 529/500 nm isosbestic ratio was negatively correlated to total Hb (r=-0.96), as was seen in the patient data. The linear fit was y=-0.007x+1, where x refers to Hb concentration and y refers to 529/500 nm reflectance ratio. The Hb saturation, which ranged from 25 to 100%, did not exhibit a strong correlation with 529/500 nm reflectance ratio (r=0.03), giving a linear fit of y=0.0001x+0.9, where x refers to Hb saturation and y refers to 529/500 nm.

Table 3. Concentrations of oxy- and deoxy-Hb and corresponding Hb saturations used in the simulations

[Oxy-Hb] (μM)	*[Deoxy-Hb] (μM)*	*[Total Hb] (μM)*	*Hb saturation (%)*
2	2	4	50
10	0	10	100
5	5	10	50
10	5	15	66.7
10	10	20	50
5	15	20	25
20	5	25	80
10	20	30	33.3
30	5	35	85.7

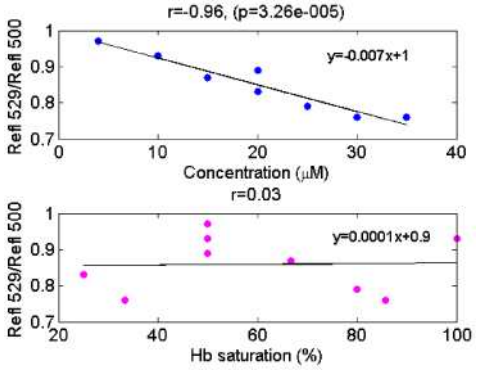

Fig. 6. Reflectance ratio at 529/500 nm versus (top) total Hb concentration and (bottom) Hb saturation.

The effect of scattering on the 529/500 nm reflectance ratio was tested for total Hb concentrations of 4, 15, 25, and 35 μM. First, μ_s'(529 nm) was fixed at 8 cm^{-1}, and then μ_s'(500 nm):μ_s'(529 nm) ratios of 1:1, 1.5:1, 2:1, and 2.5:1 were evaluated. For any given μ_s' ratio, there was a negative correlation between 529/500 nm and concentration (Fig. 7). The slopes were relatively similar for different scattering ratios, but there was a linear offset in the decay line with variation in the scattering ratio. The equations describing the linear fits for μ_s' ratios of 1, 1.5, 2, and 2.5 respectively were y=–0.006x+0.9, y=-0.007x+0.7, y=-0.004x+0.5, y=-0.004x+0.4, where x refers to the concentration and y refers to the 529/500 nm reflectance

#117329 - $15.00 USD Received 16 Sep 2009; revised 6 Nov 2009; accepted 9 Nov 2009; published 7 Dec 2009

ratio. The intercepts were roughly equal to μ_s'(529 nm):μ_s'(500 nm). The linear fits for 529/500 nm versus concentration differed slightly between Fig. 6 and for the μ_s' ratio of 1 from Fig. 7, because the ratio of μ_s' for Fig. 6 was not exactly 1:1, plus not all concentrations were used for Fig. 7.

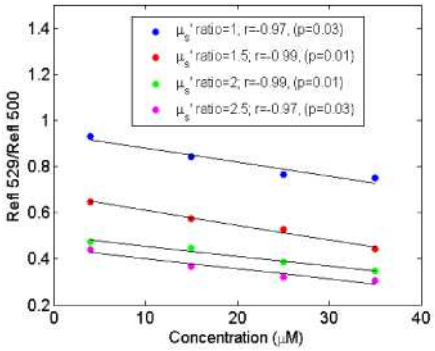

Fig. 7. Reflectance ratio of 529/500 nm versus total Hb concentration, as a function of different μ_s'(500):μ_s'(529).

4. Discussion

We show the potential to correlate simple diffuse reflectance ratios to Hb values obtained from ABG measurements during intra-operative procedures in a pilot study. It is of clinical interest to have a simple monitor that is not complex in terms of the algorithm used; this is why ratios of diffuse reflectance were evaluated. The diffuse reflectance system used here can be built more compactly, thus increasing the portability. The isosbestic ratio 529/500 nm yielded good correlations with ABG Hb, with r=-0.66. Delta comparisons, measured by subtracting the baseline for both 529/500 nm and ABG Hb, were improved, with r=-0.75. The best delta ratio was 520/509 nm, with an r=-0.84. Non-delta 520/509 correlated with ABG Hb with r=-0.61. For the first five patients alone, non-delta 529/500 nm was correlated to ABG Hb with r=-0.78. Patient #10 was shown to negatively impact the correlations the most, as determined by adding the last five patients one at a time to the first five. The correlations for individually adding patients #6-10 to patients #1-5 were r=-0.80, r=-0.79, r=-0.78, r=-0.75, and r=-0.65, respectively. If patient#10 was excluded from the total patient population, the 529/500 nm ratio was correlated to ABG Hb with r=-0.77. The delta correlation for the 520/509 nm ratio when patient #10 was excluded had r=-0.85, which is similar to the correlation when all patients were included. It is unclear at this time why patient #10 negatively impacted the non-delta correlations. In any case, delta comparisons seem to address any potential interpatient variability that might arise in the non-delta based correlations.

Diffuse reflectance ratios are expected to correlate well with Hb, because absorption of Hb is a primary source of contrast in the spectra. Isosbestic ratios are taken where the oxy- and deoxy-Hb molar extinction coefficients are equal, and so they would not be expected to correlate with the partial pressure of oxygen in the arterial plasma (PaO_2). For one of the patients, there was one PaO_2 value missing, giving a total of 35 paired optical and PaO_2 measurements. There was not a notable correlation between the isosbestic reflectance ratio of 529/500 nm and PaO_2 (r=0.25, p=0.15), indicating the isosbestic ratio is influenced by Hb but not PaO_2. The Monte Carlo simulations, carried out for a range of Hb concentrations and saturations, justify the strong negative correlation expected from the 529/500 nm reflectance ratio with total Hb (r=-0.96) and also demonstrate that this ratio is not influenced by changes in Hb saturation. When the ratio of scattering between 500 and 529 nm was varied, the 529/500 nm reflectance ratio was still negatively correlated to Hb with comparables slopes for different scattering ratios. However, the intercept of the 529/500 nm ratio was strongly

#117329 - $15.00 USD Received 16 Sep 2009; revised 6 Nov 2009; accepted 9 Nov 2009; published 7 Dec 2009

dependent on the ratio of μ_s'(529) to μ_s'(500) (r=1). For the patient data, the intercept of the experimental 529/500 nm reflectance ratio versus ABG Hb was 0.5, which was close to the averaged 529/500 nm ratio from the Spectralon reflectance standards for all 10 patients (0.4 ± 0.02). The reflectance standard is nearly spectrally flat in the wavelength range used, so the ratio effectively reflects the wavelength dependence of the system at 529 and 500 nm. It can be inferred that the intercept for the 529/500 nm ratio versus ABG Hb in the patient data would be close to unity. Based on examination of the simulation data this suggests that the scattering values in the patient data are likely very similar at 500 and 529 nm reflecting an intercept close to unity. The slope for the experimental 529/500 nm reflectance ratio versus concentration was −0.01. In the simulations, the slope was −0.006 for the μ_s' ratio of 1, which was slightly lower than the experimental ratio. Delta comparisons helped improve correlations of ratios with ABG Hb. By subtracting the baseline value in each patient, the comparisons are on the amount of change rather than on the absolute value. Given the improved correlations in the delta correlations, it can be presumed that that the non-delta ratios did not completely account for inter-patient variations in pressure.

The 529/500 nm reflectance ratio also showed potential to correct for pressure variations of the probe against the tissue surface as measured in two volunteers. When using fiber-probe based systems, it is important to take into consideration the effect of the probe-tissue interface. Several studies have shown that probe pressure has an effect on signal intensity and thus extracted parameters. One study investigating the effect of probe pressure when applied to mouse thigh muscle saw a decrease in reflectance, oxygen saturation, blood vessel radius, and Mie slope along with an increase in the reduced scattering coefficient at 700 nm with increased pressure [25]. Another study looking at the effect of pressure when applied to the rat heart and liver found that when pressure was applied the double-valley of Hb was converted to a single valley (i.e. deoxygenation) and also absorption was reduced [26]. The pressure threshold required to induce these changes in the reflectance spectra was found to be tissue-type dependent. An additional study on *ex vivo* human and animal tissue samples showed there to be a decrease in reflectance and a subsequent increase in the absorption and reduced scattering coefficient with increasing pressure [27]. To the best of our knowledge, there have been no recommendations of ways to correct for pressure-induced differences in diffuse reflectance data. Based on the volunteer study described here, the isosbestic ratio 529/500 nm appears to help account for pressure variations. The effect of pressure on other ratios was also tested, and this will be addressed more in-depth in future studies.

We have demonstrated the ability to achieve good correlations of simple diffuse reflectance ratios and blood gas parameters in a preliminary set of patient data, despite the fact that the blood gas measurements probe on the systemic level and optical measurements probe on the tissue level. The ABG measures direct concentrations of Hb in arterial blood, while diffuse reflectance measures a volume of tissue comprised of both arterial and venous components in capillary beds. The Fahraeus effect indicates the hematocrit in capillaries is generally lower than systemic hematocrit; this can be affected by capillary diameter and whether vasodilation is present [28,29]. Because of the different probing areas between optical and ABG measurements, the relationship would not necessarily be linear. Additionally, the presence of other absorbers could affect the linearity. However, the linear correlations in this study serve as a first pass at correlating regional physiological information to global Hb. The goal of this technique is to serve as a non-invasive technology for monitoring patient physiological parameters over time or guiding when ABG measurements should be drawn.

Direct measurements of tissue perfusion would be another area in which this technology may be useful. Because the probe system is measuring a volume-averaged tissue space, the measurement of acute changes in blood delivery to capillary beds would essentially be a direct measure. Studies have shown there to be a decrease in patient outcome with a decrease in gut perfusion during surgery [30]. Using optical spectroscopy intraoperatively could

#117329 - $15.00 USD Received 16 Sep 2009; revised 6 Nov 2009; accepted 9 Nov 2009; published 7 Dec 2009

potentially give real-time measurements of gut perfusion. Similarly, optical spectroscopy could be used to measure blood loss during cardiopulmonary bypass surgery, an application where pulse oximetry is not useable, due to the non-pulsatile blood flow introduced by the heart-lung bypass machine. In addition, this technology could be implemented in the assessment of the watershed blood distribution in the brain during surgery. The watershed areas in the brain are located at the most distal ends of the arteries, and thus poor perfusion can strongly impact these areas. The ability to measure the perfusion in the watershed area could perhaps decrease morbidity.

5. Conclusions

Diffuse reflectance spectra were measured from sublingual tissue in patients undergoing general surgery and in volunteers. Simple diffuse reflectance ratios were shown to correlate to Hb concentration in patients and account for variations in probe pressure in volunteers. Baseline-subtracted ratios enhanced the correlations to ABG Hb in the patient study. The methods described here are flexible, in that the instrumentation can be made more portable and the probe geometry can be custom-designed. Monte Carlo simulations supported the correlations of 529/500 nm ratio with total Hb.

Acknowledgements

This work was supported by startup funding from the Pratt School of Engineering at Duke University.

#117329 - $15.00 USD Received 16 Sep 2009; revised 6 Nov 2009; accepted 9 Nov 2009; published 7 Dec 2009